APL Materials

RESEARCH ARTICLE | MARCH 27 2023

$Li(C_2N_3)$ as eutectic forming modifier in the melting process of the molecular perovskite $[(C_3H_7)_3N(C_4H_9)]Mn(C_2N_3)_3^{\pm}$

Special Collection: Challenges and Perspectives in Materials Chemistry—A Celebration of Prof. Sir Anthony K. Cheetham's 75th Birthday

Silva M. Kronawitter ; Sebastian A. Hallweger ; Jan Meyer ; Carmen Pedri ; Stefan Burger ; Ahmad Alhadid ; Sebastian Henke ; Gregor Kieslich

APL Mater. 11, 031119 (2023)
https://doi.org/10.1063/5.0143404

AIP Publishing

$Li(C_2N_3)$ as eutectic forming modifier in the melting process of the molecular perovskite $[(C_3H_7)_3N(C_4H_9)]Mn(C_2N_3)_3$[±]

Cite as: APL Mater. 11, 031119 (2023); doi: 10.1063/5.0143404
Submitted: 23 January 2023 • Accepted: 6 March 2023 •
Published Online: 27 March 2023

Silva M. Kronawitter,[1] Sebastian A. Hallweger,[1] Jan Meyer,[1] Carmen Pedri,[1] Stefan Burger,[1] Ahmad Alhadid,[2] Sebastian Henke,[3] and Gregor Kieslich[1,a)]

AFFILIATIONS

[1] Department of Chemistry, TUM School of Natural Sciences, Technical University of Munich, Lichtenbergstraße 4, 85748 Garching, Germany
[2] Biothermodynamics, TUM School of Life Sciences, Technical University of Munich, Maximus-von-Imhof Forum 2, 85354 Freising, Germany
[3] Department of Chemistry and Biological Chemistry, Technical University of Dortmund, Otto-Hahn-Straße 6, 44227 Dortmund, Germany

Note: This paper is part of the Special Topic on Challenges and Perspectives in Materials Chemistry - A Celebration of Professor Sir Anthony K. Cheetham's 75th Birthday.
[a)] **Author to whom correspondence should be addressed:** gregor.kieslich@tum.de

ABSTRACT

Coordination polymer (CP) glasses have recently emerged as a new glass state. Given the young state of the field, the discovery of concepts that guide the synthesis of CP glasses with targeted thermal and macroscopic properties is at the center of ongoing research. In our work, we draw inspiration from research on inorganic glasses, investigating the impact of $Li(C_2N_3)$ as a modifier on the thermal properties of the new molecular perovskite $[(C_3H_7)_3N(C_4H_9)]Mn(C_2N_3)_3$ (with $[C_2N_3]^-$ = dicyanamide, DCA). We derive the phase diagram and show that $Li(C_2N_3)$ and $[(C_3H_7)_3N(C_4H_9)]Mn(C_2N_3)_3$ form a eutectic mixture, in which the melting temperature is decreased by 30 K. Additionally, for the eutectic mixture at $x_{LiDCA} \approx 0.4$, a CP glass forms under slow cooling, opening interesting pathways for scalable synthesis routes of CP glasses. Given the virtually unlimited parameter space of hybrid modifiers, they will play a major role in the future to alter the glass' properties where the availability of rigorously derived phase diagrams will be important to identify material class overarching trends.

INTRODUCTION

Coordination polymers (CPs) are composed of inorganic and organic building units, offering a large chemical space to address various applications, such as water harvesting,[1] ferroelectrics,[2] fine chemical catalysis,[3] and sensing[4] among many more. The discovery of glass-forming CPs is one of the latest milestones in the field,[5,6] conceptually closing the gap between inorganic and polymer-based glasses. Examples of glass-forming CPs are zeolitic imidazolate frameworks, such as ZIF-4 ($[Zn(Im)_2]$, Im^- = imidazolate),[7] ZIF-62 ($[Zn(Im)_{1.75}(bIm)_{0.25}]$, bIm^- = benzimidazolate),[8] and ZIF-62(M)-bIm_x[9] (M = Co^{2+}, Zn^{2+}), thiocyanate and nitrile-based CPs, such as $[Cu_2(SCN)_3(C_2bpy)]$[10] (C_2bpy^+ = 1-ethyl-[4,4-bipyridin]-1-ium) and $[Ag(mL1)(CF_3SO_3)]\cdot 2C_6H_6$ (mL1 = 1,3,5-tris(3-cyanophenylethynyl)benzene),[11] and low-dimensional CPs, such as $[Zn(HPO_4)(H_2PO_4)_2]\cdot 2H_2Im$[12] and $[Au(SPh)]_n$[13] (SPh^- = thiophenolate). In addition to the fundamental interest in this new glass-state, CP-based glasses show potential in various applied areas, such as gas separation[14] and solid electrolytes.[15,16] CP glasses are typically synthesized by rapid cooling of a melt that is obtained by heating a crystalline CP. Therefore, the melt, as a key intermediate state toward CP glasses, deserves close attention, where conceptual progress for tailoring the melting temperature (T_m) through chemical and compositional

changes to suppress parasitic decomposition processes is of great importance.[9,17,18]

More recently, a series of ABX_3 molecular perovskites $[Pr_4N]B(C_2N_3)_3$ ($[Pr_4N]^+$ = tetrapropylammonium, B = Mn^{2+}, Fe^{2+}, and Co^{2+}) was reported to melt before thermal decomposition ($T_m < T_d$) and to form a stable coordination polymer glass upon rapid cooling.[19,20] Subsequently, the manipulation of T_m by A- and B-site substitution was investigated for $AB[C_2N_3]_3$ CPs; T_m decreases with increasing alkyl chain length of the A-site cation ($[Pe_4N]^+ > [Bu_4N]^+ > [Pr_4N]^+$ with Pe = pentyl, Bu = butyl, and Pr = propyl) or decreasing Shannon ionic radius of the B-site metal ($Mn^{2+} > Fe^{2+} > Co^{2+}$).[21] A similar impact of A-site cation substitution on T_m and the glass transition temperature (T_g) was observed for 2D perovskite-related A_2BX_4 materials, such as $[A]_2PbI_4$ with six alkylammonium A-site cations (*n*-bua, *sec*-bua, 1-me-bua, *n*-hexa, 1-me-hexa, and 2-et-hexa with me = methyl, et = ethyl, bu = butyl, hex = hexyl, and a = ammonium),[22,23] despite the chemically different bonding situation within the inorganic 2D layers. These studies show that melting properties are heavily impacted by the A-site cations' entropic contributions and that B-site substitution allows for fine-tuning the materials' thermal properties. Therefore, ABX_3 perovskite-type CPs have proved as a powerful model platform for studying composition–structure–thermal property relationships by systematic compositional changes on the A-, B-, and X-site. An open opportunity that has yet not been explored for glass-forming perovskite-type materials is tailoring of glass formation properties, i.e., T_g and T_m, by the use of glass modifiers.

Our work is inspired by decades of work on inorganic glasses, where the addition of modifiers is established as a tool for tailoring glass properties,[24] i.e., their structural,[25] optical,[26] and electronic[27] properties. Recent studies on the impact of various glass-network modifiers, i.e., inorganic metal oxides (Li_2O, Na_2O, CaO, MgO, BaO, and ZnO) on the thermal properties and glass forming ability of phosphate and aluminate glasses, emphasize the suitability of this approach toward CP glass chemistry.[28,29] Additionally, it was recently shown that the superprotonic properties of $CsHSO_4$ are preserved through the formation of a binary $CsHSO_4$-CP system that shows eutectic behavior.[30] Here, we report a new molecular perovskite $[Pr_3NBu]Mn(C_2N_3)_3$, investigate its melting behavior and glass-forming ability, and explore the impact of $Na(C_2N_3)$ and $Li(C_2N_3)$ on these processes. We identify $Li(C_2N_3)$ as a suitable compound for the formation of a eutectic mixture, which stabilizes the formation of a CP glass at high amounts. Our study emphasizes that the established principles from inorganic glasses are an important research compass to unlock the potential of CP glasses, which we expect to be key in deriving CP glasses with targeted thermal properties in the future.

RESULTS AND DISCUSSION

Synthesis and thermal properties of $[Pr_3NBu]Mn(C_2N_3)_3$

In the first step, the A-site cation butyltri-*n*-propylammonium ($[Pr_3NBu]^+$) was synthesized from tri-*n*-propylamine and 1-bromobutane in a one-step nucleophilic substitution reaction, see the supplementary material (S-2) for details and Fig. S1. Single crystals of the molecular perovskite $[Pr_3NBu]Mn(C_2N_3)_3$ were obtained by following an established mild solution synthesis route by starting from $[Pr_3NBu]Br$, $MnCl_2{\cdot}6H_2O$, and $Na(C_2N_3)$ in H_2O, see Fig. S2 and the supplementary material (S-3). The structure of $[Pr_3NBu]Mn(C_2N_3)_3$ was determined via single crystal x-ray diffraction, see Fig. 1(a), Table S1, and Fig. S5 for crystallographic data. At room temperature, $[Pr_3NBu]Mn(C_2N_3)_3$ crystallizes in the space group *Pbcn* with the cell parameters a = 16.5315(17) Å, b = 17.5441(17) Å, and c = 32.348(3) Å, V = 9382.0(17) Å^3. Thermogravimetric analysis–differential scanning calorimetry (TGA–DSC) was carried out on the as-synthesized $[Pr_3NBu]Mn(C_2N_3)_3$ material, showing thermal decomposition at T_d = 570 K. Two endothermic events were observed at 371 and 474 K in the DSC signal before thermal decomposition, see Fig. S11. Variable temperature powder x-ray diffraction (VTPXRD) and cyclic DSC (Differential scanning calorimetry) measurements show that the heat event at T_{ss} = 368 K belongs to an irreversible crystalline-to-crystalline (solid-to-solid, T_{ss}) phase transition, see Fig. 1(d) and the supplementary material (Figs. S15, S16, and S26). Comparing the PXRD pattern of the high-temperature phase with the PXRD of the molecular perovskite $[Pr_3NBu]Ni(C_2N_3)_3$ suggests that both materials are isostructural. In turn, both crystalline phases of $[Pr_3NBu]Mn(C_2N_3)_3$ exhibit a perovskite-type structure motif, making $[Pr_3NBu]Mn(C_2N_3)_3$ to another molecular perovskite that shows tilt and shift polymorphism,[31] see the supplementary material (Figs. S14, S17, and S18) for details on the structure discussion. Furthermore, VTPXRD shows that the second heat event at T_m = 469.4 K, which occurs significantly before T_d, corresponds to a crystalline-to-amorphous phase transition, see Figs. 1(d) and Fig. S25. Following on from previous reports on the melting behavior of related dicyanamide-based materials,

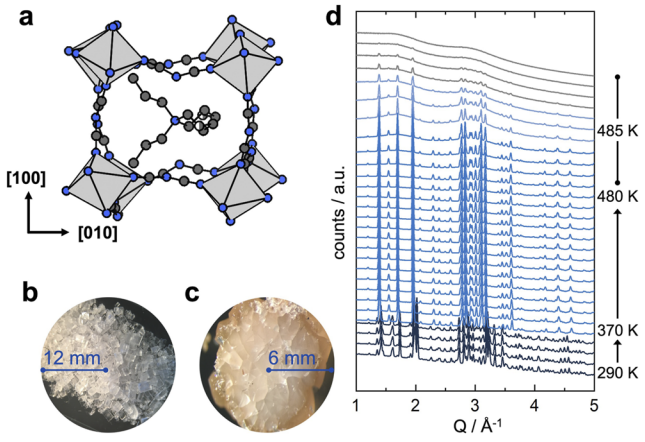

FIG. 1. (a) Structure visualization of the molecular perovskite $[Pr_3NBu]Mn(C_2N_3)_3$, where $[Mn(C_2N_3)_3]^-$ forms a 3D ReO_3-type network and the A-site molecule sits in its void for charge balance, forming the perovskite structure motif (color code: Mn polyhedral—light gray, N—dark blue, C—dark gray, and H atoms were deleted for better visualization). Optical images of the as-synthesized crystals (b) and the melt-quenched $[Pr_3NBu]Mn(C_2N_3)_3$ (c). (d) PXRD patterns (λ = 0.206 79 Å) during heating from 290 to 485 K, showing a crystalline-to-crystalline phase transition at approximately T_{ss} = 371 K (dark to light blue), followed by amorphization (gray) on holding at 485 K.

such as $[Pr_4N]Mn(C_2N_3)_3$ and $[Bu_4N]Mn(C_2N_3)_3$,[20,21,32] the second heat event is assigned to a solid-to-liquid phase transition, i.e., melting of $[Pr_3NBu]Mn(C_2N_3)_3$. This is further supported by the glass-like appearance of the melt-quenched material, see Fig. 1(c).

Melted and glassy state of $[Pr_3NBu]Mn(C_2N_3)_3$

Compared to other ABX_3 molecular perovskites, T_m = 474 K for $[Pr_3NBu]Mn(C_2N_3)_3$ is the lowest reported melting temperature to date, and the difference of ΔT = 96 K between T_d and T_m stands out being 61 K higher than for $[Pr_4N]Mn(C_2N_3)_3$ (ΔT = 35 K), see Fig. S11. However, it is important to mention that related ABX_3 non-perovskite $[C_2N_3]^-$-based CPs, such as $[Bu_4N]Mn(C_2N_3)_3$ and $[Pe_4N]Mn(C_2N_3)_3$, have been reported to melt at around 423 K.[21,32] Therefore, by drawing comparisons to ionic liquids, these results suggest describing $AB(C_2N_3)_3$ materials as $AX{\cdot}BX_2$ compounds, a perspective that highlights the inorganic–organic–ionic nature of CP melts and helps in rationalizing their thermal properties.[33] Following this train of thought, the T_m of $[Pr_3NBu]C_2N_3{\cdot}Mn(C_2N_3)_2$ agrees with previous reports: with increasing the alkyl chain length of the quaternary ammonium A-site cation, an increased entropy of melting is observed, resulting in a monotonic decrease of T_m along the series $[Pr_4N]C_2N_3{\cdot}Mn(C_2N_3)_2$ (535 K)[19,20,32] > $[Pr_3NBu]C_2N_3{\cdot}Mn(C_2N_3)_2$ (474 K) > $[Bu_4N]C_2N_3{\cdot}Mn(C_2N_3)_2$ (458 K)[21,32] > $[Pe_4N]C_2N_3{\cdot}Mn(C_2N_3)_2$ (422 K).[21,32]

Taking a closer look at the melting process of $[Pr_3NBu]Mn(C_2N_3)_3$ via cyclic DSC measurements, reversible melting is observed with a small decrease of T_m of ~4.5 K from the first cycle T_m = 469.4 K to the second cycle T_m = 464.9 K, see Fig. S26. The thermogravimetric analysis combined with mass spectrometry was used to search for potential decomposition processes during melting, see Fig. S38. No evidence for material decomposition was found up to 493.15 K, and the first fragmentation products of the A-site alkyl chain were observed at T = 513.15 K. Furthermore, ^{1}H NMR spectroscopy of the acid-digested solid after melting shows no additional signals, see Fig. S9. Therefore, decomposition processes during the melting process are expected to play a minor role if any. Slowly cooling the melt to room temperature at a rate of 5 K min^{-1} leads to recrystallization, which is observed in the DSC as a sharp exothermic event at T_c = 452.7 K, see Figs. S24 and S26. Interestingly, recrystallization after melting, which might open opportunities for new synthesis routes of functional, crystalline thin film CPs, can still be considered as an unusual behavior for CPs and has only been reported for a few examples, such as Co-bis(acetamide)[34] and Cu(isopropylimidazolate).[35] Applying a rapid cooling procedure by quenching the $[Pr_3NBu]Mn(C_2N_3)_3$ melt in liquid N_2 suppresses recrystallization and leads to x-ray amorphous, glass-like fragments, see Fig. 1(c) and Fig. S19. Elemental analysis of the melt-quenched $[Pr_3NBu]Mn(C_2N_3)_3$ agrees with the ABX_3 stoichiometry of the starting compound, see details in the supplementary material (S-5). DSC measurements of the melt-quenched $[Pr_3NBu]Mn(C_2N_3)_3$ show a glass transition at around T_g = 253.28 K, see Fig. S37. Therefore, the molecular perovskite $[Pr_3NBu]Mn(C_2N_3)_3$ forms a stable liquid upon heating and a coordination polymer glass upon rapid cooling akin to previous reports on $[Pr_4N]B(C_2N_3)_3$ (B = Mn^{2+}, Co^{2+}, and Ni^{2+}).

$Li(C_2N_3)$ as eutectic forming modifier

Drawing inspiration from research works on inorganic glasses, we investigated the impact of $M(C_2N_3)$(with M = Li^+ and Na^+) as a modifier on the melting behavior and glass formation of $[Pr_3NBu]Mn(C_2N_3)_3$. $Na(C_2N_3)$ is commercially available and was used as purchased, while $Li(C_2N_3)$ was synthesized in a modified literature procedure starting from $Na(C_2N_3)$, see preparation details in the supplementary material (S-4). The phase purity of $Li(C_2N_3)$ was confirmed by TGA–DSC analysis and IR spectroscopy, see Figs. S10 and S39–S41. Both $Li(C_2N_3)$ and $Na(C_2N_3)$ undergo a trimerization reaction upon heating while no melting is observed, see the supplementary material (S-13). Before preparation of modifier–$[Pr_3NBu]Mn(C_2N_3)_3$ mixtures of various mole ratios, both $M(C_2N_3)_3$ salts and $[Pr_3NBu]Mn(C_2N_3)_3$ were dried, see preparation details in the supplementary material (S-12). In the first step, we screened the impact of the modifier on T_m via TGA–DSC experiments of different mole fractions, see Figs. S12 and S13. From this screening series, it can be observed that the melting point of $[Pr_3NBu]Mn(C_2N_3)_3$ decreases when mixing with increasing mole fractions x_{LiDCA} of $Li(C_2N_3)$, while $Na(C_2N_3)$ as modifier has no evident impact. Applying established equations that describe the solid–liquid thermodynamics in the studied system, our experimental results suggest a large difference in theoretical melting temperatures of $Li(C_2N_3)$ and $Na(C_2N_3)$, which can be expected based on their different crystal structures; for a more elaborate discussion, see the supplementary material (S-37).

Subsequently, we explored the impact of $Li(C_2N_3)$ on T_m as a function of increasing mole fractions x_{LiDCA} (x_{LiDCA} = 0, 0.15, 0.25, 0.32, 0.38, 0.41, 0.45, 0.49, 0.58, and 0.66) via DSC in more detail, see Fig. 2 and Figs. S27–S35. From the DSC traces, it is evident that an increase in x_{LiDCA} has no significant impact on T_{ss} of

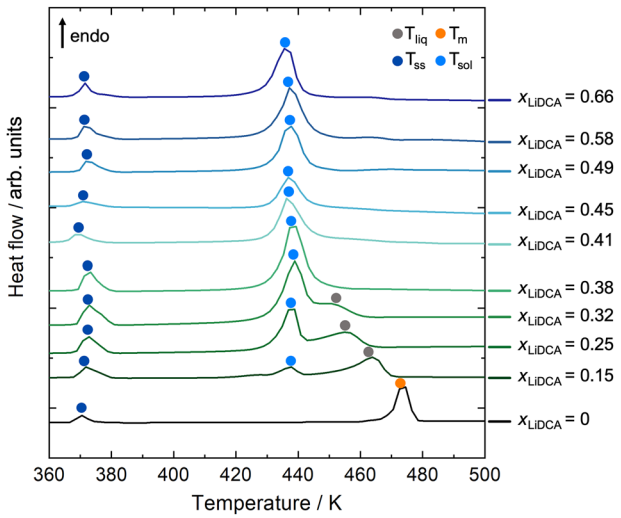

FIG. 2. DSC curves of $Li(C_2N_3)$–$[Pr_3NBu]Mn(C_2N_3)_3$ mixtures with varying the amount of modifier salt, x_{LiDCA}. The DSC data of various mole fractions obtained on heating were used to build a phase diagram. For better visualization, the curves are offset by a random shift.

$[Pr_3NBu]Mn(C_2N_3)_3$. This is expected as there is no obvious pathway of how $Li(C_2N_3)$ as a modifier impacts the internal structural reorganization of $[Pr_3NBu]Mn(C_2N_3)_3$ prior to melting. In contrast, already at x_{LiDCA} = 0.15, two distinct endothermic signals become visible in the DSC traces, which belong to the liquidus (T_{liq}) and the solidus temperature (T_{sol}), see Fig. S27. Further increasing x_{LiDCA} leads to a monotonic decrease of T_{liq} until approximately x_{LiDCA} ≈ 0.4, where the eutectic mixture (T_{sol} = T_{liq}) is reached. Furthermore, in the second heating cycle of the mixtures x_{LiDCA} = 0.15, 0.25, 0.32, and 0.38, an exothermic event is observed, see Figs. S27–S30. This exothermic event reflects a structural reorganization related to crystallization and is known as cold crystallization (T_{cc}). Overall, for x_{LiDCA} = 0.38, a decrease of ~30 K in the melting of the homogeneous mixture (T_{liq}) is observed; for comparison purposes with literature data, the offset temperature of T_m is used for the discussion, while Table S3 contains both T_m as determined from peak onset and offset. Taken together, the data provide the basis to build a temperature–composition phase diagram up to x_{LiDCA} = 0.41, see Fig. 3. To the best of our knowledge, this is the first report of a molecular perovskite-related eutectic mixture, showcasing the applicability of established concepts to tailor the thermal properties of melting coordination polymers.

The decreased T_m of $[Pr_3NBu]Mn(C_2N_3)_3$ by the formation of a eutectic mixture with $Li(C_2N_3)$ as a modifier provides improved opportunities for glass formation compared to currently employed TGA–DSC-based processes. Additionally, opening the gap between T_m and T_d is expected to further suppress any potential decomposition processes. To demonstrate this, we performed simple model experiments by heating 20 mg of mixtures near the eutectic (x_{LiDCA} = 0.38 and 0.41) to 443 or 441 K in a glass vial under Ar atmosphere, see method details in the supplementary material (S-5). Initial melting started after 10 min, and after 30 min, the melting process was completed. After cooling slowly to room temperature, the remaining solids were transparent and had a drop-like appearance, see Fig. S4. Comparing the PXRD pattern prior to and after melting of the mixture closest to the eutectic (x_{LiDCA} = 0.41), all sharp reflections disappeared, see Fig. S23. For the mixture of x_{LiDCA} = 0.38, however, evidence for crystalline domains remained, which is expected from the observed recrystallization event in the DSC traces of the x_{LiDCA} = 0.38 mixture when cooled slowly, see Figs. S21, S22, and S30. Importantly, an excess of $Li(C_2N_3)$ (x_{LiDCA} = 0.41 and higher) avoids any recrystallization even when cooled slowly. This suggests that the composition of the eutectic mixture is at a mole fraction of approximately x_{LiDCA} ≈ 0.4. In parallel, for all mixtures with a mole fraction x_{LiDCA} ≥ 0.41–0.66, a clear glass transition T_g is visible, which decreases from T_g = 312.3 K (x_{LiDCA} = 0.41) to T_g = 301.3 K (x_{LiDCA} = 0.66), see Figs. S31–S35. Furthermore, miscibility of $[Pr_3NBu]Mn(C_2N_3)_3$ and $Li(C_2N_3)$ in the liquid state is assumed since only a single T_g was obtained for mixtures between x_{LiDCA} = 0.41 and 0.66, see Figs. S31–S35. Therefore, $Li(C_2N_3)$ is a suitable modifier for tailoring the melting behavior of the molecular perovskite $[Pr_3NBu]Mn(C_2N_3)_3$.

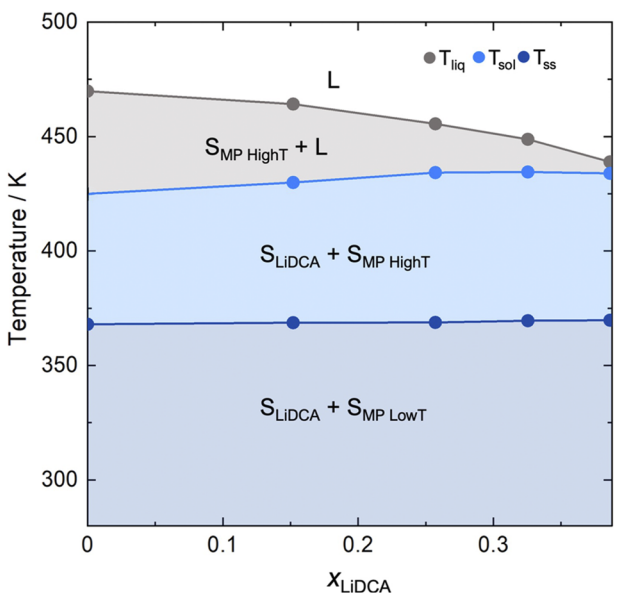

FIG. 3. Partial phase diagram of the binary$Li(C_2N_3)$–$[Pr_3NBu]Mn(C_2N_3)_3$ system at ambient pressure showing simple eutectic behavior, with S = solid phase, L = liquid phase, MP = molecular perovskite, and LiDCA = $Li(C_2N_3)$. We would like to note that the phase diagram was built from DSC data of the initial heating run up to x_{LiDCA} = 0.41 since T_{liq} of mixtures with higher mole fractions (x_{LiDCA} = 0.41, 0.45, 0.49, 0.58, 0.66) are not possible to determine. For small mole fractions, we observed a very weak signal without a clear peak onset and offset, and for larger mole fractions, we assume that T_{liq} raises quickly above the temperature where trimerization of $Li(C_2N_3)$ and/or decomposition of $[Pr_3NBu]Mn(C_2N_3)_3$ start.

CONCLUSION

We report the synthesis of the new molecular perovskite $[Pr_3NBu]Mn(C_2N_3)_3$, investigate its melting behavior, and show that $Li(C_2N_3)$ is a suitable eutectic forming glass modifier. For the eutectic mixture at x_{LiDCA} ≈ 0.4, we observe a decrease of T_m of 30 K and show that a CP glass can be obtained even when cooled slowly. Our results underpin that established principles for inorganic glasses are a suitable compass for progressing the area of CP glasses, and specifically, the use of eutectic mixtures provides a myriad of opportunities to alter the glass' resulting macroscopic properties.

In going forward, the use of "non-innocent" glass modifiers, i.e., modifiers with an intrinsic physical property, such as optical activity or interesting photophysics, might offer a pathway to incorporate new properties in the resulting glass beyond its impact as a modifier *per se*. For instance, for an AX modifier, A^+ might be optical active while X^- guarantees high miscibility with the parent material when chosen according to the chemistry of the glass forming CP. Additionally, we propose that established formulas that describe the underlying solid–liquid thermodynamics can guide the search for other potential eutectic formers for CP forming glasses such as purely organic $[C_2N_3]^-$-based modifier salts with suitable melting temperatures for $[C_2N_3]^-$-based molecular perovskites. Future research opportunities include the investigation of materials' mechanical properties, such as compressibility, bulk moduli, and thermal expansion behavior, as a function of mole fractions x_{LiDCA}. Therefore, we believe that the use of modifiers will become an increasingly important research branch in the field of CP glasses, for which our results provide an important fundamental groundwork.

SUPPLEMENTARY MATERIAL

See the supplementary material for the complete material synthesis, characterization and thermal analysis of the studied perovskite, modifier salts, and perovskite–modifier mixtures.

DEDICATION

Dedicated to the 75th Birthday of A. K. Cheetham.

ACKNOWLEDGMENTS

We like to thank Alba S. J. Méndez and Martin Etter for their support during data collection at Beamline P02.1 at the Deutsche Elektronensynchrotron DESY (PETRA III, Hamburg, Germany). G.K. gratefully thanks the Fonds der Chemischen Industrie and the DFG (Project No. 450070835) for financial support.

AUTHOR DECLARATIONS

Conflict of Interest

The authors have no conflicts to disclose.

Author Contributions

Silva M. Kronawitter: Data curation (equal); Formal analysis (equal); Investigation (equal); Methodology (equal); Validation (equal); Visualization (equal); Writing – original draft (equal). **Sebastian A. Hallweger**: Data curation (equal); Investigation (equal). **Jan Meyer**: Investigation (equal). **Carmen Pedri**: Investigation (equal). **Stefan Burger**: Investigation (equal); Writing – review & editing (equal). **Ahmad Alhadid**: Data curation (equal); Investigation (equal); Writing – review & editing (equal). **Sebastian Henke**: Validation (equal); Writing – review & editing (equal). **Gregor Kieslich**: Conceptualization (equal); Funding acquisition (equal); Project administration (equal); Resources (equal); Supervision (equal); Writing – review & editing (equal).

DATA AVAILABILITY

The data that support the findings of this study are available within the supplementary material.

REFERENCES

[1] H. Kim, S. Yang, S. R. Rao, S. Narayanan, E. A. Kapustin, H. Furukawa, A. S. Umans, O. M. Yaghi, and E. N. Wang, Science **356**, 430 (2017).
[2] Y.-M. Xie, J.-H. Liu, X.-Y. Wu, Z.-G. Zhao, Q.-S. Zhang, F. Wang, S.-C. Chen, and C.-Z. Lu, Cryst. Growth Des. **8**, 3914 (2008).
[3] L. Jiao, Y. Wang, H.-L. Jiang, and Q. Xu, Adv. Mater. **30**, 1703663 (2018).
[4] L. E. Kreno, K. Leong, O. K. Farha, M. Allendorf, R. P. van Duyne, and J. T. Hupp, Chem. Rev. **112**, 1105 (2012).
[5] T. D. Bennett and S. Horike, Nat. Rev. Mater. **3**, 431 (2018).
[6] S. Horike, S. S. Nagarkar, T. Ogawa, and S. Kitagawa, Angew. Chem., Int. Ed. **59**, 6652 (2020).
[7] T. D. Bennett, J.-C. Tan, Y. Yue, E. Baxter, C. Ducati, N. J. Terrill, H. H.-M. Yeung, Z. Zhou, W. Chen, S. Henke, A. K. Cheetham, and G. N. Greaves, Nat. Chem. **6**, 8079 (2015).
[8] T. D. Bennett, Y. Yue, P. Li, A. Qiao, H. Tao, N. G. Greaves, T. Richards, G. I. Lampronti, S. A. T. Redfern, F. Blanc, O. K. Farha, J. T. Hupp, A. K. Cheetham, and D. A. Keen, J. Am. Chem. Soc. **138**, 3484 (2016).
[9] L. Frentzel-Beyme, M. Kloß, P. Kolodzeiski, R. Pallach, and S. Henke, J. Am. Chem. Soc. **141**, 12362 (2019).
[10] S. S. Nagarkar, H. Kurasho, N. T. Duong, Y. Nishiyama, S. Kitagawa, and S. Horike, Chem. Commun. **55**, 5455 (2019).
[11] C. Das, T. Ogawa, and S. Horike, Chem. Commun. **56**, 8980 (2020).
[12] D. Umeyama, S. Horike, M. Inukai, T. Itakura, and S. Kitagawa, J. Am. Chem. Soc. **137**, 864 (2015).
[13] S. Vaidya, O. Veselska, A. Zhadan, M. Diaz-Lopez, Y. Joly, P. Bordet, N. Guillou, C. Dujardin, G. Ledoux, F. Toche, R. Chiriac, A. Fateeva, S. Horike, and A. Demessence, Chem. Sci. **11**, 6815 (2020).
[14] Y. Wang, H. Jin, Q. Ma, K. Mo, H. Mao, A. Feldhoff, X. Cao, Y. Li, F. Pan, and Z. Jiang, Angew. Chem., Int. Ed. **59**, 4365 (2020).
[15] T. Ogawa, K. Takahashi, S. S. Nagarkar, K. Ohara, Y.-L. Hong, Y. Nishiyama, and S. Horike, Chem. Sci. **11**, 5175 (2020).
[16] N. Ma, S. Kosasang, A. Yoshida, and S. Horike, Chem. Sci. **12**, 5818 (2021).
[17] H. Kimata and T. Mochida, Chem. - Eur. J. **25**, 10111 (2019).
[18] M. Lusi, Cryst. Growth Des. **18**, 3704 (2018).
[19] B. K. Shaw, A. R. Hughes, M. Ducamp, S. Moss, A. Debnath, A. F. Sapnik, M. F. Thorne, L. N. McHugh, A. Pugliese, D. S. Keeble, P. Chater, J. M. Bermudez-Garcia, X. Moya, S. K. Saha, D. A. Keen, F.-X. Coudert, F. Blanc, and T. D. Bennett, Nat. Chem. **13**, 778 (2021).
[20] J. M. Bermúdez-García, M. Sánchez-Andújar, S. Yáñez-Vilar, S. Castro-García, R. Artiaga, J. López-Beceiro, L. Botana, Á. Alegría, and M. A. Señarís-Rodríguez, Inorg. Chem. **54**, 11680 (2015).
[21] B. K. Shaw, C. Castillo-Blas, M. F. Thorne, M. L. Ríos Gómez, T. Forrest, M. D. Lopez, P. A. Chater, L. N. McHugh, D. A. Keen, and T. D. Bennett, Chem. Sci. **13**, 2033 (2022).
[22] A. Singh, M. K. Jana, and D. B. Mitzi, Adv. Mater. **33**, 2005868 (2021).
[23] T. Li, W. A. Dunlap-Shohl, E. W. Reinheimer, P. Le Magueres, and D. B. Mitzi, Chem. Sci. **10**, 1168 (2019).
[24] J. Lu, Z. Shan, J. Zhang, Y. Su, K. Yi, Y. Zhang, and Q. Zheng, J. Non-Cryst. Solids: X **16**, 100125 (2022).
[25] N. Ghribi, M. Dutreilh-Colas, J.-R. Duclère, T. Hayakawa, J. Carreaud, R. Karray, A. Kabadou, and P. Thomas, J. Alloys Compd. **622**, 333 (2015).
[26] A. Marzuki and D. E. Fausta, IOP Conf. Ser.: Mater. Sci. Eng. **858**, 012035 (2020).
[27] B. Roling and M. D. Ingram, J. Non-Cryst. Solids **265**, 113 (2000).
[28] Y. He, X. Shen, Y. Jiang, and A. Lu, Mater. Chem. Phys. **258**, 123865 (2021).
[29] K. Griebenow, C. B. Bragatto, E. I. Kamitsos, and L. Wondraczek, J. Non-Cryst. Solids **481**, 447 (2018).
[30] N. Ma, N. Horike, L. Lombardo, S. Kosasang, K. Kageyama, C. Thanaphatkosol, K. Kongpatpanich, K.-I. Otake, and S. Horike, J. Am. Chem. Soc. **144**, 18619 (2022).
[31] S. Burger, S. Grover, K. T. Butler, H. L. B. Boström, R. Grau-Crespo, and G. Kieslich, Mater. Horiz. **8**, 2444 (2021).
[32] J. A. Schlueter, J. L. Manson, and U. Geiser, Inorg. Chem. **44**, 3194 (2005).
[33] J. Dupont, Acc. Chem. Res. **44**, 1223 (2011).
[34] M. Liu, A. H. Slavney, S. Tao, R. D. McGillicuddy, C. C. Lee, M. B. Wenny, S. J. L. Billinge, and J. A. Mason, J. Am. Chem. Soc. **144**, 22262 (2022).
[35] T. Watcharatpong, T. Pila, T. Maihom, T. Ogawa, T. Kurihara, K. Ohara, T. Inoue, H. Tabe, Y.-S. Wei, K. Kongpatpanich, and S. Horike, Chem. Sci. **13**, 11422 (2022).